EPR and ^{129}Xe NMR Studies of Copper-Exchanged NaY Zeolites†

Shang-Bin Liu,*,‡ Tien-Sung Lin,*,§ Tran-Chin Yang,‡ Tung-Ho Chen,‡ Eng-Chin Hong,‡,|| and Ryong Ryoo⊥

Institute of Atomic and Molecular Sciences, Academia Sinica, P.O. Box 23-166, Taipei, Taiwan 10764, Republic of China, Department of Chemistry, Washington University, St. Louis, Missouri 63130, and Department of Chemistry, Korea Advanced Institute of Science and Technology, Taeduk Science Town, Taejon 305-701, Korea

Received: November 15, 1994; In Final Form: February 20, 1995⊗

In side-by-side EPR and ^{129}Xe NMR studies, the occupancy sites of Cu^{2+} ions in copper-exchanged NaY zeolites are found to depend on the state of reduction/oxidation cycle, the concentration of Cu^{2+} ions, the sample temperature, and the adsorbate present in the zeolites. The structural features of Y zeolites in the presence of Xe, He, H_2, and O_2 under various reduction and oxidation conditions are examined carefully by these two spectroscopic techniques. The EPR spectral features of Cu^{2+} in the presence of O_2 adsorbate vary as a function of temperature. The temperature dependence study allows us to calculate the activation energy of migration of Cu^{2+} from small cages to supercages, which is found to be 9.7 ± 0.8 kJ/mol. A model is proposed to explain the spectral changes.

Introduction

There have been many spectroscopic studies of the copper-exchanged NaY zeolites, especially EPR studies.[1−10] Most of these EPR experiments were performed at or below 77 K and on samples treated under various different conditions. Since the spectral features of Cu^{2+} in Y zeolites are influenced by the degree of hydration, the temperature and duration of heat treatment, and the nature of cations in the zeolite, the reported EPR spectral parameters varied from one study to another. Recently, we reported some peculiar behaviors of ^{129}Xe NMR results in the dehydrated Cu^{2+}-exchanged Y zeolites: the chemical shifts depend linearly on the xenon loading and are unaffected by the original copper concentration in the CuNaY samples.[11] These NMR behaviors differ from those of other transition metal ions under similar experimental conditions. Moreover, it has been indicated that prolonged dehydration at elevated temperatures can lead to autoreduction.[12,13] These prompted us to perform detailed EPR and ^{129}Xe NMR studies, side-by-side, on samples with varied copper concentrations under different treatment conditions, and in the presence of different gaseous adsorbates, such as Xe, He, H_2, and O_2, so that the electronic nature of copper ions in CuNaY zeolites could be fully characterized. Some of the spectral features observed in our EPR experiments differ from those reported previously, especially those in the presence of O_2 adsorbate. A model is proposed to explain the observed spectral changes which correlate well with the results obtained from isotherm and ^{129}Xe NMR measurements of xenon adsorbed in various CuNaY samples.

Experimental Section

The preparation and characterization of CuNaY samples with different exchanged Cu^{2+} concentrations: 5, 13, 28, 35, 49, and 57% (denoted CuNaY-5, CuNaY-13, etc.) and the related details of the ^{129}Xe NMR experiments were given previously.[11]

The sample tube configuration was designed so that a 5 mm standard quartz tube joined to a stopcock could be conveniently set up on a vacuum apparatus for adsorption or desorption of various adsorbates, isolation, or further thermal and oxidation/reduction treatments of the sample. Dehydration of the CuNaY sample was achieved by continuous evacuation to 3×10^{-3} Pa at 673 K for at least 20 h until autoreduction took place to ensure a complete dehydration which was monitored by EPR runs. It has been reported that the "autoreduction" can result from a hydrocarbon background in the vacuum system.[13] However, we have taken extreme precautions to use greaseless stopcocks to avoid such an effect.

Progressive oxidation (or reduction) of the samples took place in the presence of 9×10^4 Pa of O_2 (or H_2) gas over a temperature range of 423−673 K for a period of 2−8 h. A prolonged reduction process normally resulted in a mixture of Cu^+ and Cu^0 in the CuNaY sample judging from the coloration of the sample and the negative EPR spectra.

An X-band EPR spectrometer (Bruker ER 300) equipped with variable temperature unit was employed in our measurements. A sample of diphenylpicrylhydrazyl (DPPH; $g = 2.0037$) was used as the g-value marker. All the NMR spectra were taken immediately after the EPR spectra of the samples were measured. Such side-by-side measurements of magnetic properties allow us to examine closely the electronic nature of each particular sample.

Results and Discussion

(A). EPR Studies. *(1). Temperature Effects of O_2 Adsorbed CuNaY.* To circumvent the possible complication of the concentration effect, the temperature dependence EPR experiments were performed on the most diluted sample, namely, CuNaY-5. The EPR spectra of Cu^{2+} in the presence of O_2 gas as a function of temperature are displayed in Figure 1. At 300 K, it seems to consist of two sets of spectra: an intense set and a weak broad one. We employed a Bruker software package to fit the observed spectra. We found that the set of intense lines exhibits rhombic symmetry with the following spin

† Presented, in part, at the 10th International Zeolite Conference, Garmisch-Partenkirchen, Germany, July 1994.
‡ Academia Sinica.
§ Washington University.
|| Permanent address: Department of Chemical Engineering, Chenghsiu Junior College of Technology, Kaohsiung, Taiwan 83305, ROC.
⊥ Korea Advanced Institute of Science and Technology.
⊗ Abstract published in *Advance ACS Abstracts,* April 15, 1995.

0022-3654/95/2099-8277$09.00/0

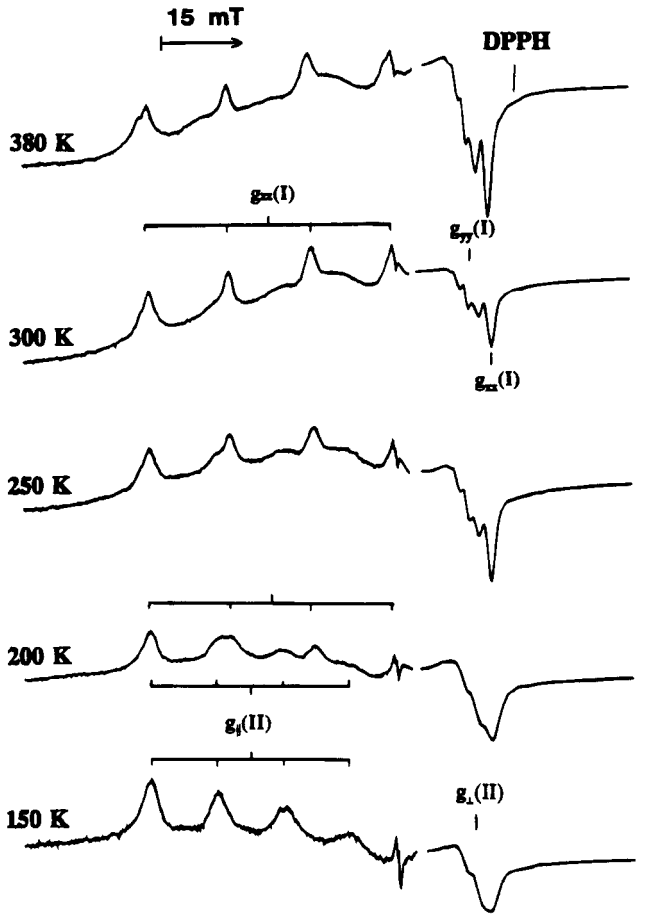

Figure 1. EPR spectra of Cu^{2+} in ion-exchanged CuNaY-5 zeolite as a function of temperature in the presence of O_2 gas (9×10^4 Pa). The gain in the $g_{\|}$ spectral region is five times greater than that in the $g_{\perp}$ region.

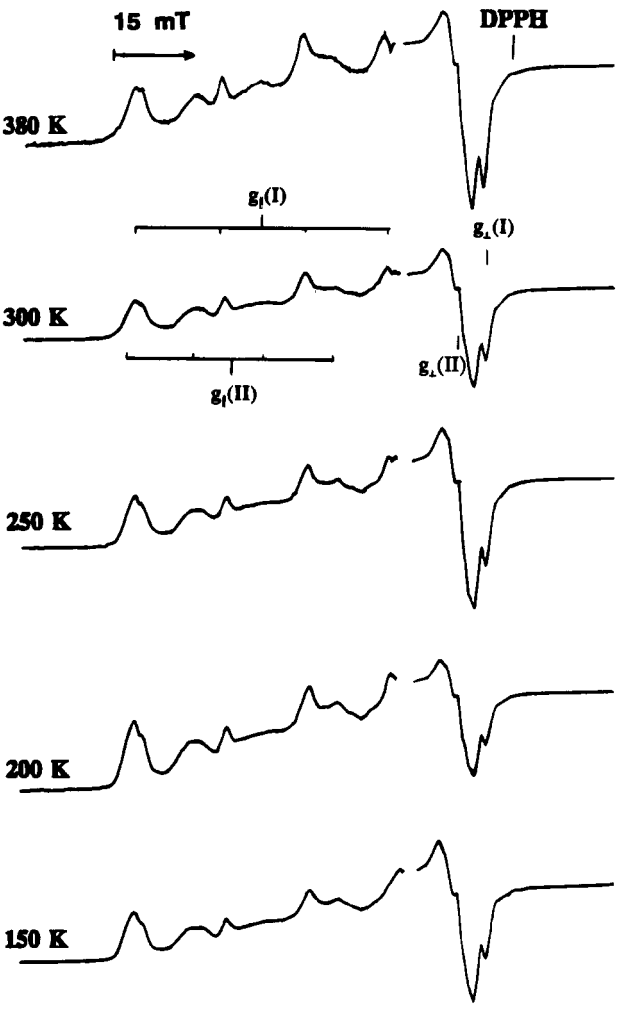

Figure 2. EPR spectra of Cu^{2+} in ion-exchanged CuNaY-5 zeolite as a function of temperature in vacuum. The gain in the $g_{\|}$ spectral region is five times greater than that in the $g_{\perp}$ region.

Hamiltonian parameters: $g_{zz} = 2.334$, $g_{yy} = 2.066$, and $g_{xx} = 2.036$; $A_{zz} = 15.5$, $A_{yy} = 1.6$, and $A_{xx} \approx 0$ mT. The estimated errors are ± 0.005 for the g-values and ± 0.2 mT for the hyperfine splitting. The intense lines at high temperature indicate that Cu^{2+} ions are in a nonaxial symmetry environment, possibly in a distorted trigonal potential field formed in the Si–O–Al framework.

The set of weak broad spectral lines gradually gain intensity as temperature is lowered and become dominant at 180 K. Finally, at 150 K, the set of intense lines observed at high temperature disappears completely. The low-temperature spectral pattern has axial symmetry with the following parameters: $g_{\|} = 2.363$ and $g_{\perp} = 2.070$; $A_{\|} = 12.1$ and $A_{\perp} = 0.5$ mT. At low temperatures, the axially symmetric EPR spectra with greater g-values and smaller hyperfine splittings would mean that Cu^{2+} in the presence of O_2 is in the hexagonal prisms, similar to previously reported EPR results.[1]

We further notice that an equilibrium exists between two sets of spectral lines in Figure 1: one set gains intensity at the expense of the other as temperature varies. The spectral changes are reversible and reproducible in the heating and cooling cycles of the sample.

The spectral changes as a function of temperature may arise from the following factors: (1) paramagnetic effect of O_2 on Cu^{2+}, (2) change of lattice constants, or (3) migration of Cu^{2+} to different sites. If factor 1 prevails due to spin-dipolar or spin-exchange interaction of O_2 and Cu^{2+}, we would expect to observe a change of spectral line width as a function of temperature. In fact, oxygen broadening of Cu^{2+} spectra has been reported for paramagnetic centers located in the supercages of the Y zeolites.[9,10] However, upon careful examination of Figure 1, we have not noticed any changes of line width in a given spectral set at any temperature. Thus we may rule out the contribution of paramagnetic effect.

To address the possible effect of factor 2, we performed another set of EPR experiments on the same sample with oxygen removed by evacuation (at 3×10^{-3} Pa). The EPR spectra of Cu^{2+} in the absence of O_2 as a function of temperature are displayed in Figure 2. We have not observed any spectral changes in the temperature range of 150 to 380 K. Therefore we may rule out factor 2: the lattice effects. Thus, the spectral changes displayed in Figure 1 may arise from factor 3, migration of Cu^{2+} from the hexagonal prism at low temperature outward toward the supercages. In other words, the adsorption of O_2 in the cavity could affect the occupancy sites and the electronic configuration of Cu^{2+} ions.

Furthermore, Figure 2 consists of two sets of spectral parameters at all temperatures which may be assigned to different Cu^{2+} configurations: set I, $g_{\|}(I) = 2.332$ and $g_{\perp}(I) = 2.035$, $A_{\|}(I) = 15.6$ and $A_{\perp}(I) \approx 0$ mT; set II, $g_{\|}(II) = 2.365$ and $g_{\perp}(II) = 2.065$, $A_{\|}(II) = 12.0$ and $A_{\perp}(II) = 1.0$ mT. Note that the intensities of set II are relatively weak and broad. The spectral parameters of Figure 1 and 2 are summarized in Table 1.

Moreover, in these temperature dependence studies, we found that the integrated spectral intensity remains the same throughout

TABLE 1: Spectral Parameters of CuNaY Samples

			set I		set II	
sample	adsorbate	T (K)	g	A (mT)	g	A (mT)
CuNaY-5	O_2	150			2.070	0.5
					2.363	12.1
	O_2	380	2.036	~0		
			2.066	1.6		
			2.334	15.5		
	none	300	2.035	~0	2.064	1.0
			2.332	15.6	2.365	12.1
CuNaY-13	none	300	2.035	~0	2.062	1.0
			2.331	15.8	2.365	12.1
CuNaY-28	none	300	2.034	~0		
			2.067	1.7	2.061	1.0
			2.331	15.6	2.368	12.4
CuNaY-35	none	300	2.035	~0		
			2.068	1.5	2.062	1.0
			2.336	15.7	2.365	12.6
CuNaY-57	none	300	2.034	~0		
			2.066	1.6	2.063	
			2.337	15.6	2.372	12.5

the entire temperature range. Thus the spin concentration of the sample remains unchanged.

It has been indicated that the Cu^{2+} ions are located in the supercages in the hydrated CuNaY zeolite, but the Cu^{2+} ions can migrate into small cages during the dehydration process.[1,9,10,13] In the completely dehydrated NaY zeolite, Cu^{2+} ions are bound to oxygen atoms in the Si−O−Al framework and located in the small cages, either at site SI (in the centers of hexagonal prisms) or at offset sites SI′ (in the surroundings of hexagonal prisms which project into the sodalite cage from the shared six-membered rings).[9] In fact, X-ray diffraction studies showed that there are 14−16 Cu^{2+} ions per unit cell located preferentially at SI and SI′ sites.[14-16] In a recent temperature-programmed desorption (TPD) experiments of the dehydrated CuNaY zeolite exposed to O_2, five different modes of oxygen adsorption were observed.[14,17] The oxygen adsorbates responsible for TPD peaks are bound directly or indirectly by the cations in the zeolite. It has been indicated that O_2 is mostly located in the supercages at room temperature and could enter the small cages at or above 573 K.

At first glance, it seems that the high-temperature spectra of the oxygenated sample may be attributed to the binding of O_2 (located in supercages) to Cu^{2+}. However, in the concentration dependence studies (*vide infra*), we observed the same spectra in the properly treated highly Cu^{2+} exchanged samples in the absence of oxygen.

The observed equilibrium between the high- and low-temperature spectra would further lend support to the proposed migration of Cu^{2+} from hexagonal prisms toward supercages upon increasing temperature, i.e., more Cu^{2+} ions interact with O_2 (located in the supercage) at higher temperatures. Here, we assume O_2 cannot enter small cages at or below 380 K.[14,17] From the measurements of intensity ratios of one of the copper hyperfine components ($m = {}^1/_2$) of the two sets of spectral lines displayed in Figure 1 as a function of temperature, we obtain the heat of activation (migration), $\Delta H = 9.7 \pm 0.8$ kJ/mol (Figure 3). This is the first time, to the best of our knowledge, that the activation energy involving migration of Cu^{2+} from small cages to supercages under the influence of O_2 adsorbate has been obtained.

To further support this argument, we have performed EPR studies on the same CuNaY sample in the presence of other gases, such as Xe, He, or H_2, under similar conditions. We found the shape and the splittings of the EPR spectra of Cu^{2+} ions in the presence of these gases remains unchanged regardless of the sample temperature. Thus, we may conclude that the

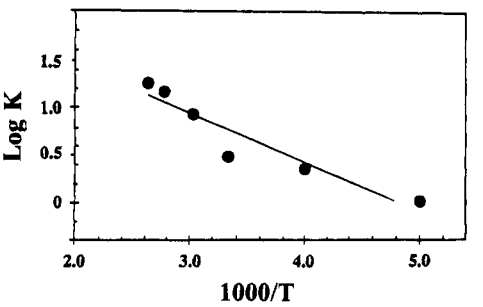

Figure 3. A plot of hyperfine intensity ($m = {}^1/_2$) ratios of set I and set II (from Figure 1) vs $1/T$.

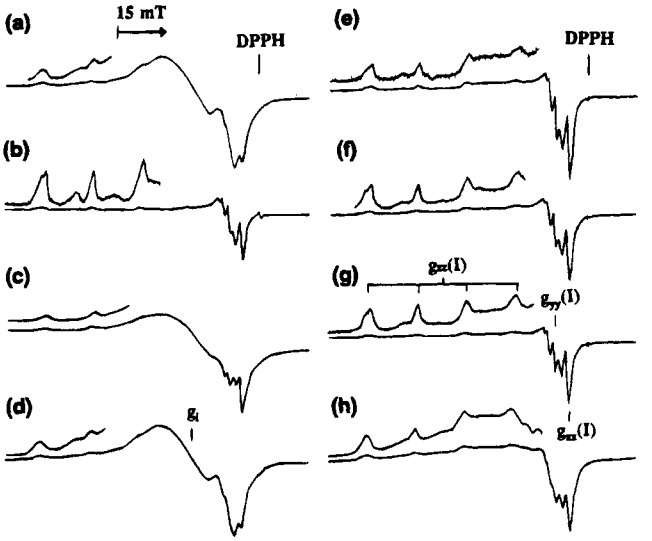

Figure 4. Room temperature EPR spectra of Cu^{2+}. (a−f) For CuNaY-28 samples during the reduction/oxidation cycle: (a) dehydration under vacuum at 673 K for 48 h; (b) reduction with H_2 at 9×10^4 Pa and 573 K for 4 h; (c) oxidation with O_2 at 9×10^4 Pa and 673 K for 4 h (in the presence of O_2); (d) removal of O_2; (e) final reduction with H_2 at 9×10^4 Pa and 453 K for 2 h (in the presence of H_2); (f) removal of H_2; (g) for CuNaY-35, same condition as (f); (h) for CuNaY-57, same condition as (f). The upper traces (in the $g_{||}$ region) of each spectrum are expanded 5−10 times in intensity.

presence of O_2 in the zeolite supercages can modify the location of Cu^{2+} even at room temperature.

(2). Concentration Effects. It was found that the concentration of Cu^{2+} could be controlled by the degree of reduction/oxidation conditions regardless of the initial copper contents.[1] However, the occupancy sites of Cu^{2+} (EPR detectable) may depend on the degree of reduction/oxidation of a given CuNaY sample. Therefore, we performed a series of spectroscopic studies concerning the Cu^{2+} concentration effects. We attempted to examine the electronic nature of the cupric ions in the reduction/oxidation processes as a function of the initial concentration of the Cu^{2+}-exchanged CuNaY zeolites.

The room temperature EPR spectra of the CuNaY-28 sample that underwent the complete reduction/oxidation cycle are displayed in Figure 4. The spectra were taken at each of the following redox steps: (a) dehydration under vacuum at 673 K for 48 h, (b) reduction with H_2 at 9×10^4 Pa and 573 K for 4 h, (c) oxidation with O_2 at 9×10^4 Pa and 673 K for 4 h (in the presence of O_2), (d) removal of O_2, (e) final reduction with H_2 at 9×10^4 Pa and 453 K for 2 h (in the presence of H_2), and (f) removal of H_2.

The broad intense isotropic peak with $g_i = 2.16$ observed in spectra 4a,c,d is attributed to the pairwise interaction between Cu^{2+} ions in the strongly oxidized state. Such spectral features have been reported previously.[1,4] We would like to point out

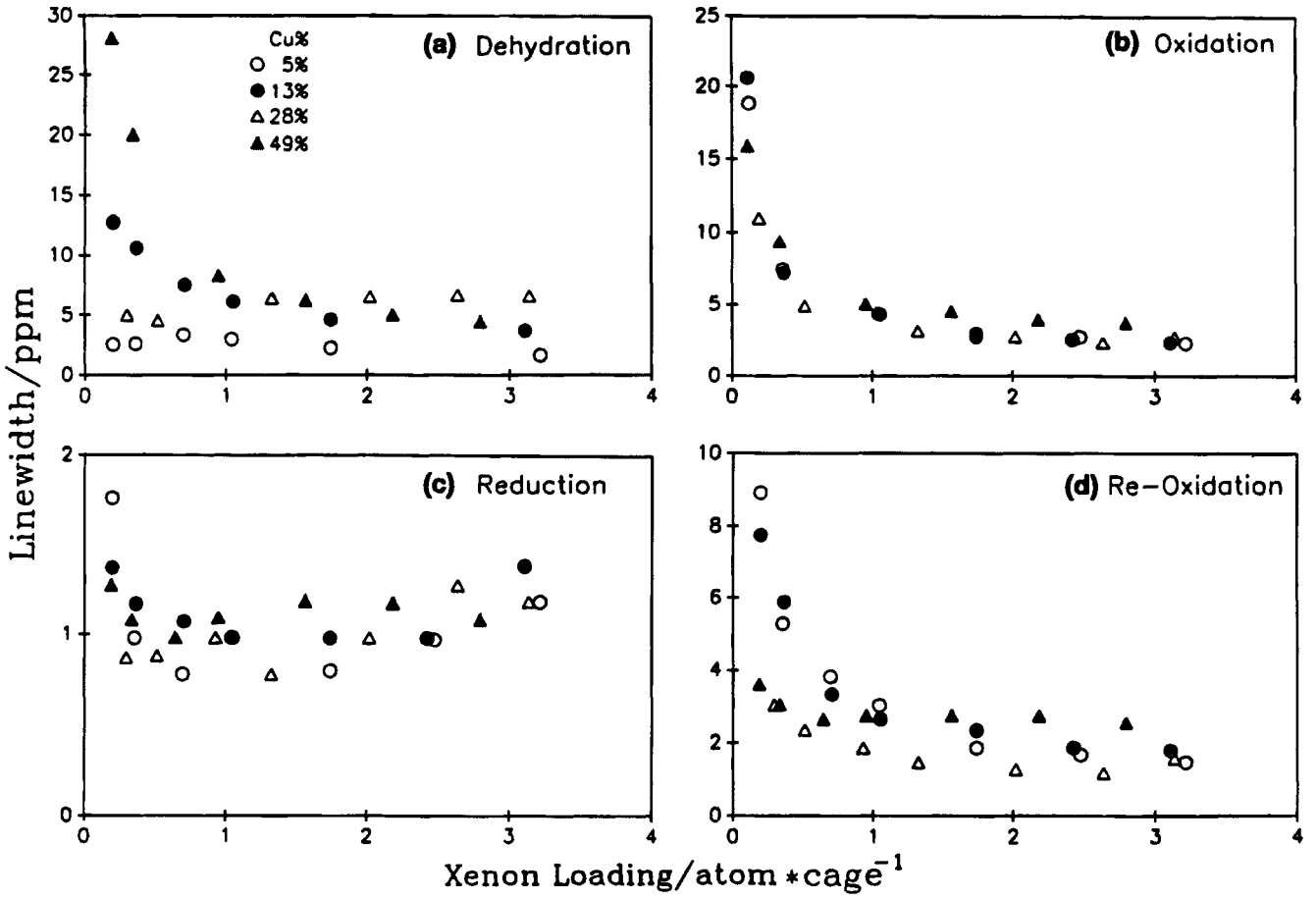

Figure 5. The variations of ^{129}Xe NMR line widths *vs* Xe loading for various percent Cu^{2+}-exchanged CuNaY zeolites: (a) dehydrated state; (b) oxidized state; (c) reduced state; and (d) reoxidized state.

the spectral difference in the $g_\perp$ region between spectrum 4c (in the presence of O_2) and spectrum 4d (in vacuum): the presence of O_2 affects the spectral feature even in the high Cu^{2+} content sample. The spectral features are similar to those of CuNaY-5 displayed in Figure 1. We note that the presence of O_2 does not affect or induce spectral broadening (except slightly broadening in the g_i region), other than the additional spectral hyperfine splittings that appear in spectrum 4c. We further note that the spectral features remain the same regardless of the presence or absence of H_2 gas (*cf.* spectra 4e,f).

To confirm the effect, we have examined other higher concentration samples: 35 and 57% copper-exchanged NaY zeolites under similar sample treatment conditions. The spectra (corresponding to the redox step of spectrum 4f in the absence of any adsorbates) are displayed in 4g,h. The spectral features of 4e–h (all in the absence of O_2) are the same as those of Figure 1 at high temperatures in the presence of O_2 adsorbate. Thus the species corresponding to the spectra observed at high temperature for CuNaY-5 in the presence of O_2 and that observed at room temperature for high copper content samples without O_2 have the same configuration.

It has been suggested that the rate-limiting step in the reduction (oxidation) process is the migration of Cu^{2+} (Cu^+) ions from small cages to supercages.[1,13] Furthermore, it was suggested that Cu^+ ions can easily migrate back into small cages after the reduction process. It appears that the reduction/oxidation processes mainly take place in the supercages. Also in high copper content samples, some of Cu^{2+} are located in supercages as indicated in the conduction measurements.[18] Thus it is plausible the Cu^{2+} site corresponding to the spectra observed at high temperature for CuNaY-5 in the presence of O_2 adsorbate (Figure 1), and spectra 4b,e–h are the same and are most likely located in the sodalite cages or in the peripherals of supercages.

The spectral parameters for all of the systems we have studied are summarized in Table 1. In general, there are two sets of spectral lines with the following average parameters: set I, $g_{zz} = 2.335$, $g_{yy} = 2.067$, and $g_{xx} = 2.035$, $A_{zz} = 15.6$, $A_{yy} = 1.6$, and $A_{xx} \approx 0$ mT; set II, $g_{\parallel}(II) = 2.367$ and $g_\perp(II) = 2.064$, $A_{\parallel}(II) = 12.4$ and $A_\perp(II) \approx 1.0$ mT. The spectral behaviors of CuNaY samples during the redox cycle for different copper contents are summarized as follows:

(1). Prolonged dehydration of the sample at elevated temperatures can lead to autoreduction.

(2). Reduction in the presence of H_2 at elevated temperatures can effectively reduce the Cu^{2+} ions to Cu^+ or even metallic copper regardless of the original Cu^{2+} concentration. However, the distribution of Cu^{2+} ions in various cavity sites depends on the original concentration.

(3). Under proper oxidation condition, we were able to reproduce both the low- and high-temperature-oxygenated spectra of Figure 1 for any samples. From the EPR results, we may conclude that Cu^{2+} ions prefer to locate in smaller cages. When these sites are fully occupied, the cupric ions will then extend outward to supercages. The reduction/oxidation processes take place in the supercages at high temperature. But the copper ions will migrate back to the small cages after the redox. This observation is seemingly in accord with the "memory effect" proposed by Herman and Flentge.[1]

(4). At high temperatures, the Cu^{2+} ions are constantly hopping from site to site, and, given enough time, they will migrate into the supercage where they can interact with O_2 adsorbate. Once the interaction occurs, the mobility of Cu^{2+}

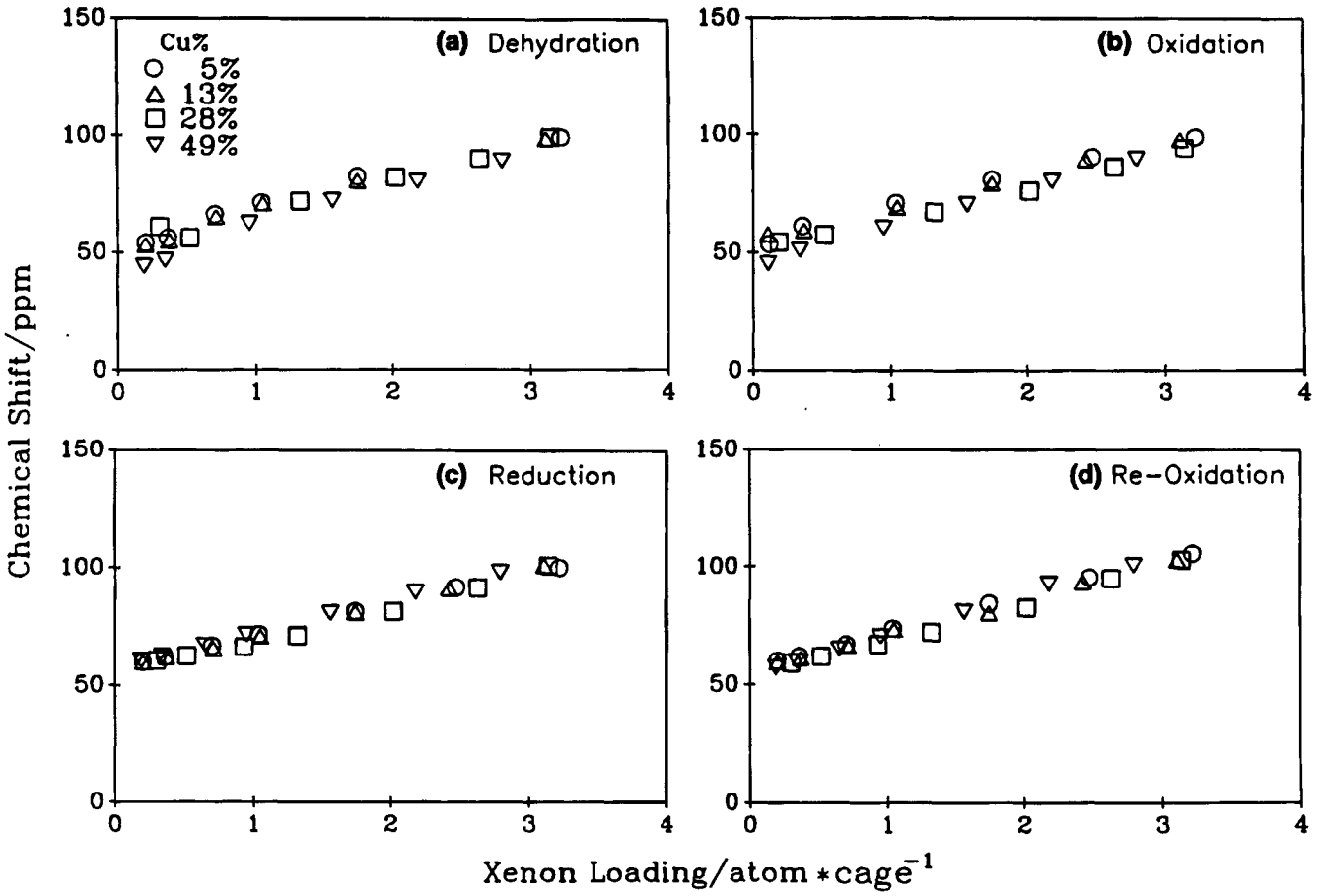

Figure 6. ^{129}Xe NMR chemical shift *vs* Xe loading for various concentration of CuNaY zeolites: (a) dehydrated state; (b) oxidized state; (c) reduced state; and (d) reoxidized state.

ions will be restricted as indicated in the temperature dependence studies. Similar migration of Cu^{2+} in the presence of other attractive adsorbates has also been reported in the X-ray diffraction study.[15]

(B). ^{129}Xe NMR Studies. The line width and chemical shifts of ^{129}Xe NMR spectra in Y zeolites are known to be very sensitive to the presence of paramagnetic ions and their occupancy sites.[11] We have performed detailed ^{129}Xe NMR studies along with the EPR studies for each of the samples so that we can examine the nature of paramagnetic effect on ^{129}Xe NMR spectra. We summarize our NMR findings as follows:

(1). ^{129}Xe NMR Line Width. The dependence of the ^{129}Xe line width on xenon loading for various CuNaY samples under different redox conditions are displayed in Figure 5.

(a). Dehydrated State. We observed that the line width varies somewhat irregularly with Cu^{2+} contents (Figure 5a). This implies that partial reduction can take place in the dehydrated CuNaY, confirming our EPR observation. The sharp increase in line width at low xenon loading for the samples with high copper contents, such as 49%, is likely due to the presence of paramagnetic Cu^{2+} ions in the supercage or in its peripheral (see also EPR spectrum, Figure 4a). Upon increasing Xe loading, the Xe−Xe interactions become dominant and cause the linewidth to decrease to ca 5 ppm. However, some minor paramagnetic effect of the dehydrated state is recognizable when one compares with the totally reduced state: 5 vs 1 ppm at high Xe loading (*cf.* Figure 5c).

(b). Oxidized State. The line width for the controlled oxidized samples (after the complete reduction in the dehydration step) appear to be independent of Cu^{2+} content (Figure 5b). All of the samples show an increase in line width at low Xe loading. The line width decreases to ca. 4 ppm at high Xe loading. Since the size of Xe atom is too large to enter the smaller cages, direct contact between Xe and Cu^{2+} should be negligibly small in all cases.

The larger line width at low Xe loading may arise from two factors: (1) some paramagnetic effect (*cf.* Figure 5a−c) and (2) a wider frequency distribution as the Xe atom at very low loading will be free to migrate from cage to cage and experience slight differences in its environment and therefore a broader line width. One further notes that the increase in line width at decreasing Xe loading has also been observed in other Y zeolites, even in the parent NaY.[11] On the other hand, at higher Xe loading, the Xe atoms will begin to interact with each other and give rise to an average local field of nuclear spins and therefore a narrower line width. The interaction between them should be at most through space, e.g., via Coulombic or dipole−dipole interactions. Again the residual line width at higher Xe loading is similar to the dehydrated state.

(c). Reduced State. The amount of Cu^{2+} present in the samples should be very low except for the very high percent Cu^{2+}-exchanged samples, such as CuNaY-49, where a weak EPR spectrum was still observed. As shown in Figure 5c, the maximum line width at very low Xe loading is not more than 2 ppm (*vs.* >20 ppm in conditions a and b), and it falls to about 1 ppm, which is similar to that of parent NaY (prior to the Cu^{2+} exchange). These values are all smaller than those of dehydrated and oxidized state given above. Thus, we may conclude that most of the copper ions are now in the reduced state, Cu^{+}, which can interact weakly with Xe via the diamagnetic effect.

(d). Reoxidized State. The reoxidized state was obtained immediately after the second reduction step. Again, we observed an increase of ^{129}Xe line width at low Xe loading (Figure 5d), and the overall line width decrease to ca. 2 ppm at higher Xe loading. These values are less than those observed in the partially dehydrated and the former oxidized states (*cf.* Figure 5a,b). The decrease in residual line width would imply that the Cu^{2+} ions may be distributed more uniformly than the former oxidized state. Also, the number of Cu^{2+} ions present in the peripheral of supercage may be less than those in conditions a and b.

In summary, the paramagnetic effect due to Cu^{2+} on the ^{129}Xe line width is pronounced at low Xe loading, but relatively small at high Xe loading, at most 4 ppm. This is in contrast to that observed in other paramagnetic ions, such as Ni^{2+} and Co^{2+} in NaY zeolites.[11,22] Nevertheless, the small paramagnetic effect of Cu^{2+} in the NMR experiments is consistent with the results of our EPR studies.

(2). ^{129}Xe NMR Chemical Shifts. The variations of ^{129}Xe NMR chemical shift with Xe loading for various CuNaY samples under different redox conditions are displayed in Figure 6. We summarize the results of ^{129}Xe chemical shift as follows:

(a). Effect of Xe Concentration. A linear dependence between chemical shifts and Xe concentration is observed. The linear relationship can be expressed as[11]

$$\delta = \delta_0 + \delta_s + \delta_{em} + \sigma_{Xe}\varrho_{Xe} \quad (1)$$

where $\delta_0 = 0$ ppm is the reference, δ_s corresponds to the shift arising from the Xe−zeolite wall interactions in the absence of the Xe−Xe interactions (i.e., $\sigma_{Xe}\varrho_{Xe} = 0$), δ_{em} represents the electromagnetic effect due to the presence of the paramagnetic ions, and the last term is the Xe−Xe interaction which changes linearly with its density, ϱ_{Xe}.

Extrapolating the chemical shift data to zero Xe loading (i.e., $\varrho_{Xe} = 0$), we obtained the following intercepts ($\delta_s + \delta_{em}$): 50 ppm for redox conditions a and b and 55 ppm for conditions c and d. We may set $\delta_{em} = 0$ for the sample being void of paramagnetic ions, i.e., in the reduced state (Figure 6c), and take the intercept of Figure 6c to be δ_s (=55 ppm) for the CuNaY system. This value should be compared with $\delta_s \approx 57$ ppm found in parent NaY. According to the simple mean-free-path theory of Ito and Fraissard,[19,20] a smaller δ_s value at zero Xe loading would imply that Xe atom experiences a greater mean-free-path and hence reflects a greater free volume of the zeolite supercage.

If $\delta_s = 55$ ppm for the CuNaY samples, we obtain $\delta_{em} = -5$ ppm for conditions a and b where the presence of paramagnetic ions have been verified in the EPR studies. The observation of a negative δ_{em} value is a peculiar effect, even though it has been reported in a similar system.[21] Further experiments are needed to explore the origin of this peculiar effect.

(b). Effect of Cu^{2+} Content. The relationship is independent of Cu^{2+} content and the sample treatment conditions. An averaged slope $\sigma_{Xe} \approx 14.96$ ppm·cage·atom^{-1} is obtained. This value is somewhat similar to that for parent NaY value (15.31 ppm·cage·atom^{-1}), suggesting that the mechanism of Xe−Xe interaction remains almost unchanged upon Cu^{2+} ion exchange.

On the other hand, in a previous NMR study, the intercepts are 47 ppm for a 57% copper-exchanged Y zeolite, and 58 ppm for 5% copper content.[11] Again a negative δ_{em} value is indicated in an independent study.

Conclusion

The detailed side-by-side EPR and ^{129}Xe NMR studies of Cu^{2+} exchanged CuNaY zeolites with different concentrations and redox conditions allow us to examine the electronic structure and occupancy sites of cupric ions in Y zeolites. This combined magnetic resonance studies also enable us to investigate the reduction/oxidation processes in a stepwise fashion. Our temperature dependence EPR studies demonstrate that the presence of high affinity adsorbates, such as O_2, could affect the occupancy sites of cupric ions in CuNaY zeolites, i.e., Cu^{2+} could migrate from the hexagonal prism sites outward to the supercages if enough thermal energy is provided.

Acknowledgment. This work is supported partially by the National Science Council (NSC), R.O.C. (NSC83-0208-M001-092, SBL) and partially by National Science Foundation (CHE-9106499, T.S.L.). T.S.L. acknowledges the support of the NSC for a Visiting Professorship at IAMS. We thank Prof. T.-I. Ho and Mr. C.-H. Wang for technical assistance in using the EPR spectrometer.

References and Notes

(1) Herman, R. G.; Flentge, D. R. *J. Phys. Chem.* **1978**, *82*, 720 and references therein.
(2) Flentge, D. R.; Lunsford, J. H.; Jacobs, P. A.; Uytterhoeven, J. B. *J. Phys. Chem.* **1975**, *79*, 354.
(3) Herman, R. G.; Lunsford, J. H.; Beyer, H.; Jacobs, P. A.; Uytterhoeven, J. B. *J. Phys. Chem.* **1975**, *79*, 2388.
(4) Chao, C. C.; Lunsford, J. H. *J. Chem. Phys.* **1972**, *57*, 2890.
(5) Vansant, E. F.; Lunsford, J. H. *J. Phys. Chem.* **1972**, *76*, 2860.
(6) Maxwell, I. E.; Drent, E. *J. Catal.* **1976**, *41*, 412.
(7) Slot, H. B.; Verbeek, J. L. *J. Catal.* **1969**, *12*, 216.
(8) Conesa, J. C.; Soria, J. *J. Phys. Chem.* **1978**, *82*, 1575.
(9) Ichikawa, T.; Kevan, L. *J. Phys. Chem.* **1983**, *87*, 4433.
(10) Turkevich, J.; Ono, Y.; Soria, J. *J. Catal.* **1972**, *25*, 44.
(11) (a) Liu, S.-B.; Fung, B.-F.; Yang, T.-C.; Hong, E.-C.; Chang, C.-T.; Shih, P.-C.; Tong, F.-H.; Chen, T.-L. *J. Phys. Chem.* **1994**, *98*, 4393. (b) Liu, S.-B.; Yang, T.-C.; Lin, R.-Y.; Hong, E.-C.; Lin, T.-S. *Stud. Surf. Sci. Catal.* **1994**, *84*, 789.
(12) Kasai, P. H.; Bishop, R. J. *J. Phys. Chem.* **1977**, *81*, 1527.
(13) (a) Jacobs, P. A.; De Wilde, W.; Schoonheydt, R. A.; Uytterhoeven, J. B. *J. Chem. Soc., Faraday Trans.* **1976**, *72*, 1221. (b) Jacobs, P. A.; Tielen, M.; Linart, J.-P.; Uytterhoeven, J. B.; Beyer, H. *J. Chem. Soc., Faraday Trans.* **1976**, *72*, 2793.
(14) Iwamoto, M.; Maruyama, K.; Yamazoe, N.; Selyama, T. *J. Phys. Chem.* **1977**, *81*, 622.
(15) Gallezot, P.; Ben Tarrit, Y.; Imelik, B. *J. Catal.* **1972**, *26*, 295.
(16) Maxwell, I. E.; de Boer, J. J. *J. Phys. Chem.* **1975**, *79*, 1874.
(17) Iwamoto, M.; Nakamura, M.; Nagano, H.; Kagawa, S.; Selyama, T. *J. Phys. Chem.* **1982**, *86*, 153.
(18) Schoonheydt, R. A.; Velghe, F. *J. Chem. Soc., Faraday Trans.* **1976**, *72*, 172.
(19) Fraissard, J.; Ito, T.; de Menorval, L. C.; Springuel-Huet, M. A. *Stud. Surf. Sci. Catal.* **1982**, *12*, 179.
(20) Ito, T.; Fraissard, J. P. *J. Chem. Soc., Faraday Trans. 1* **1987**, *83*, 451.
(21) Boddenberg, B.; Hartmann, M. *Chem. Phys. Lett.* **1993**, *203*, 243.
(22) Liu, S.-B.; Yang, T.-C.; Lin, T.-S. Unpublished results.

JP943057E